

## Supplementary Information

### **Tumor-targeted near-infrared fluorophore for fluorescence-guided phototherapy**

Min Ho Park,<sup>a</sup> Gayoung Jo,<sup>b</sup> Eun Jeong Kim,<sup>b</sup> Jin Seok Jung,<sup>b</sup> and Hoon Hyun\*<sup>b</sup>

<sup>a</sup> Department of Surgery, Chonnam National University Medical School, Gwangju 61469, South Korea

<sup>b</sup> Department of Biomedical Sciences, Chonnam National University Medical School, Gwangju 61469, South Korea

\* To whom correspondence should be addressed. Email: hhyun@jnu.ac.kr

#### **Contents:**

##### **Experimental details**

**Fig. S1** (a) Mass spectrum and (b) optical property of the CA800SO3 NIR fluorophore.

**Fig. S2** Live cancer cell binding of CA800SO3 in NCI-H460, MCF-7, MDA-MB-231, and HT-29 cells.

**Fig. S3** Time-dependent biodistribution of CA800SO3 NIR fluorophore.

## Experimental details

**Synthesis of CA800SO3 NIR fluorophore.** All chemicals and solvents were of American Chemical Society grade or HPLC purity. Starting materials were purchased from Sigma-Aldrich (St. Louis, USA) and were used without purification. 2,3,3-trimethylindolenine-5-sulfonic acid **1** (1 g, 4.2 mmol) and bromoacetic acid **2** (0.87 g, 6.2 mmol) in toluene (50 mL) was heated at 100 °C for 72 h under a nitrogen atmosphere. The mixture was cooled to room temperature and the solvent was decanted. The crude mixture was washed with acetonitrile and ethyl acetate. The collected solid was used directly in the next step without further purification (0.55 g, 44%). A mixture of heterocyclic salt **3** (0.1 g, 0.33 mmol), Vilsmeier-Haack reagent **4** (0.06 g, 0.16 mmol), and anhydrous sodium acetate (0.04 g, 0.48 mmol) in absolute ethanol (5 mL) was heated under reflux for 6 h. The reaction mixture was cooled to ambient temperature, and then dried by rotovap to remove the reaction solvent, and purified as a dark-green solid **5** (CA800SO3; 0.05 g, 42%). The final product **5** was separated by using a preparative HPLC system equipped with a 150 mL PrepLC fluid handling unit, a manual injector (Rheodyne 7725i), and a 2487 dual wavelength absorbance detector (Waters, Milford, USA). The molecular weight of the purified sample was measured by mass spectroscopy using an ultra-performance liquid chromatography (UPLC, Waters) device equipped with micrOTOF-Q II (Bruker, Germany).

**Optical property analysis.** All the optical measurements were performed in phosphate-buffered saline (PBS) at pH 7.4. Absorbance and fluorescence emission spectra of CA800SO3 were measured using a fiber optic flame absorbance and fluorescence (200–1025 nm) spectrometer (Ocean Optics, Dunedin, USA). Molar extinction coefficient was calculated by using the Beer-Lambert equation. To determine the fluorescence quantum yield, indocyanine green (ICG) dissolved in dimethyl sulfoxide (DMSO) (quantum yield = 13%) was used as a calibration standard under the conditions of matched absorbance at 770 nm.<sup>1,2</sup> An NIR excitation light source was provided by 5 mW of 655 nm red laser pointer (Opcom Inc., Xiamen, China) which was coupled with a 400  $\mu\text{m}$  core diameter, NA 0.22 fiber (Ocean Optics).

***In vitro* photothermal conversion efficiency.** Based on the equation reported previously,<sup>3,4</sup> the photothermal conversion efficiency ( $\eta$ ) of the CA800SO3 NIR fluorophore was calculated as follows:

$$\eta = \frac{hA\Delta T_{\max} - Q_s}{I(1 - 10^{-A_\lambda})}$$

where  $h$  is the heat transfer coefficient,  $A$  is the surface area of the container,  $\Delta T_{\max}$  is the temperature change of the sample solution at the maximum temperature,  $I$  is the laser power density,  $A_\lambda$  is the absorbance of sample at 808 nm, and  $Q_s$  is the heat associated with the light absorbance of the solvent.

***In vitro* reactive oxygen species (ROS) generation assay.** The ROS generation of CA800SO3 NIR fluorophore was determined from the fluorescence signals of Singlet Oxygen Sensor Green® reagent (SOSG, Thermo Fisher Scientific, Waltham, USA), following the manufacturer's instructions. CA800SO3 was added to SOSG solutions (10  $\mu$ M in phosphate-buffered saline, PBS, pH 7.4) for the final concentrations of 2.5–20  $\mu$ M CA800SO3, respectively. Then, the mixtures were irradiated with an 808 nm laser (1.1 W/cm<sup>2</sup>) for 1 min. SOSG fluorescence ( $\lambda_{\text{ex}}/\lambda_{\text{em}} = 488/525$  nm) was monitored by the FOBI imaging system (NeoScience, Suwon, South Korea). The quantification of <sup>1</sup>O<sub>2</sub> generation efficiency ( $\Phi\Delta$ ) of CA800SO3 are estimated by comparing the photosensitizing reaction rate of CA800SO3 with that of ICG used as the reference by the following equation:  $\Phi\Delta_{\text{CA800SO3}} = (r_{\text{CA800SO3}}/A_{\text{CA800SO3}})/(r_{\text{ICG}}/A_{\text{ICG}}) \times \Phi\Delta_{\text{ICG}}$ , where  $r_{\text{CA800SO3}}$  and  $r_{\text{ICG}}$  are the SOSG reaction rate with <sup>1</sup>O<sub>2</sub> generated from CA800SO3 and ICG, which can be directly obtained from time-dependent fluorescence enhancement of SOSG, respectively;  $A_{\text{CA800SO3}}$  and  $A_{\text{ICG}}$  are the corresponding absorbances of CA800SO3 and ICG at 808 nm, respectively;  $\Phi\Delta_{\text{ICG}}$  is the known <sup>1</sup>O<sub>2</sub> generation efficiency of ICG, which is 0.2%.<sup>5</sup>

***In vitro* cancer cell binding and NIR fluorescence microscopy.** The human large-cell lung carcinoma cell line (NCI-H460), the human breast adenocarcinoma cell lines (MCF-7 and MDA-MB-231), and the human colorectal adenocarcinoma cell line (HT-29) were obtained from the American Type Culture Collection (ATCC, Manassas, USA). The cancer cells were maintained in RPMI 1640 medium (Gibco BRL, Paisley, UK) supplemented with 10% fetal bovine serum (FBS, Gibco BRL) and an antibiotic-antimycotic solution (100 units/mL penicillin, 100  $\mu$ g/mL streptomycin, and 0.25  $\mu$ g/mL amphotericin B; Welgene, Daegu, South Korea) in a humidified 5% CO<sub>2</sub> atmosphere at 37 °C. When the cells reached approximately 50% confluence, they were then rinsed twice with PBS, and the CA800SO3 NIR fluorophore was added to each well at a concentration of 2  $\mu$ M, and cells were incubated for 1 h at 37 °C. They were then gently washed

with PBS. NIR fluorescence imaging was performed using a 4-filter set on a Nikon Eclipse Ti-U inverted microscope system. The microscope was equipped with a 100 W halogen lamp, NIR-compatible optics, and a NIR-compatible 10X Plan Fluor objective lens (Nikon, Seoul, South Korea). Image acquisition and analysis were performed using NIS-Elements Basic Research software (Nikon). NIR filter sets composed of  $750 \pm 25$  nm excitation filters, 785 nm dichroic mirrors, and  $810 \pm 20$  nm emission filters were used to detect NIR fluorescence signals in cancer cells. All NIR fluorescence images were acquired at identical exposure times and normalized.

**NCI-H460 xenograft mouse model.** Animal care, experiments, and subsequent euthanasia were performed in accordance with protocols approved by Chonnam National University Animal Research Committee (CNU IACUC-H-2017-64). Six-week old adult male NCRNU nude mice weighing approximately 25 g ( $N = 3$  independent experiments) were purchased from Orient (Seongnam, South Korea). NCI-H460 cancer cells ( $1 \times 10^6$  cells per mouse) were harvested and suspended in 100  $\mu$ L PBS followed by subcutaneous injection in the right flank of each mouse. When the tumor size reached about 1 cm in diameter, CA800SO3 was administered intravenously. Animals were euthanized and imaged over a certain period of time.

***In vivo* tumor imaging.** *In vivo* NIR fluorescence imaging was performed using the Mini-FLARE<sup>®</sup> imaging system as described previously.<sup>6</sup> Briefly, the system consisted of separate light sources of different wavelengths: a “white” LED light source generating 26,600 lux of 400–650 nm light to illuminate the surgical field, an NIR LED light source generating 7.70 mW/cm<sup>2</sup> of 745–779 nm fluorescence excitation light. Additionally, *in vivo* SOSG fluorescence at 525 nm was monitored by the FOBI imaging system (NeoScience). Fluorescence intensities accumulated in tumors were analyzed using ImageJ version 1.45q. All fluorescence images were normalized identically for all conditions. To confirm the *in vivo* antitumor effect, the macroscopic morphologies in each group were observed at determined time intervals for a week. The tumor volumes were calculated using the following formula:  $V = 0.5 \times \text{longest diameter} \times (\text{shortest diameter})^2$ .

***In vivo* photothermal effect assessment.** NCI-H460 tumor mice were intravenously administered with PBS or CA800SO3. The mice were anaesthetized 24 h after injection, and the tumors were irradiated by laser (1.1 W/cm<sup>2</sup>,  $\lambda = 808$  nm) for 5 min. Temperature changes in the

tumors were monitored by using a FLIR® thermal imager (FLIR Systems, Wilsonville, USA). Data were recorded starting from the beginning of the laser irradiation with a step-size of 1 min during the whole laser irradiation period. At 24 h post-irradiation, tumors were excised from the treated mice for subsequent histological analysis using hematoxylin and eosin (H&E) staining.

**Statistical analysis.** Statistical analysis was carried out using a one-way ANOVA followed by Tukey's multiple comparisons test. Differences were considered to be statistically significant at a level of  $p < 0.05$ . Results were presented as mean  $\pm$  S.D. and curve fitting was performed using Prism version 4.0a software (GraphPad, San Diego, USA).

**Histological analysis.** Resected tumors were preserved for H&E staining and microscopic assessment. Samples were fixed in 2% paraformaldehyde and flash frozen in optimal cutting temperature (OCT) compound using liquid nitrogen. Frozen samples were cryosectioned (10  $\mu$ m in thickness per slide), stained with H&E, and observed by microscopy. Histological imaging was performed on a Nikon Eclipse Ti-U inverted microscope system. Image acquisition and analysis was performed using NIS-Elements Basic Research software (Nikon).

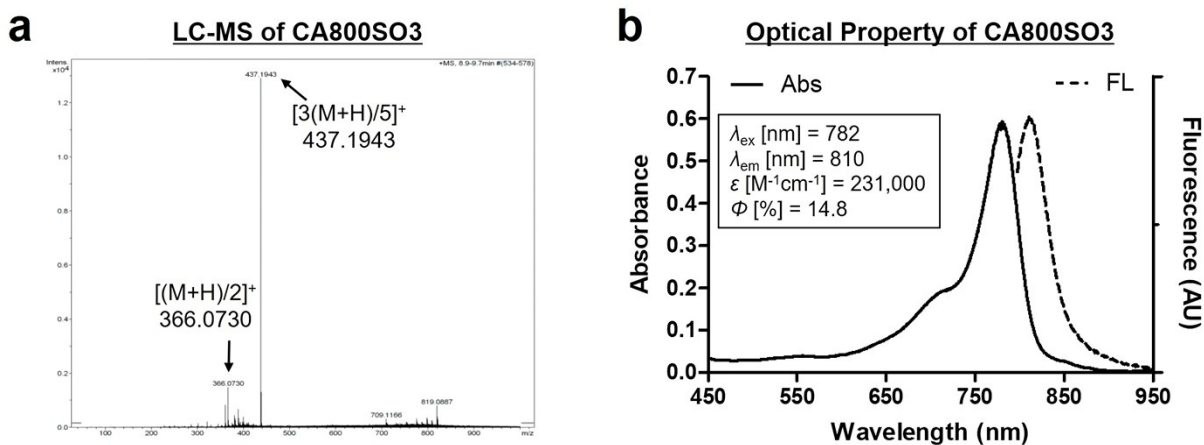


**Fig. S1** (a) Mass spectrum and (b) optical property of the CA800SO3 NIR fluorophore. Optical measurements were performed in PBS, pH 7.4.

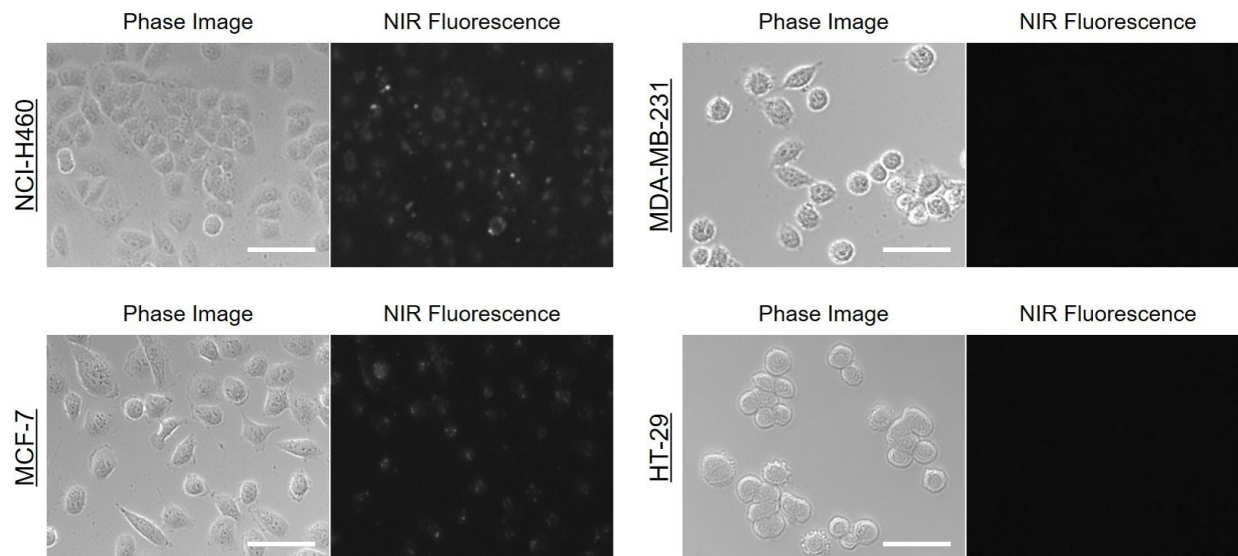


**Fig. S2** Live cancer cell binding of CA800SO3 in NCI-H460, MCF-7, MDA-MB-231, and HT-29 cells. Phase and NIR fluorescence images of each cell lines were obtained at a concentration of 2  $\mu$ M. Images are representative of three independent experiments. All NIR fluorescence images have identical exposure and normalizations. Scale bars = 50  $\mu$ m.

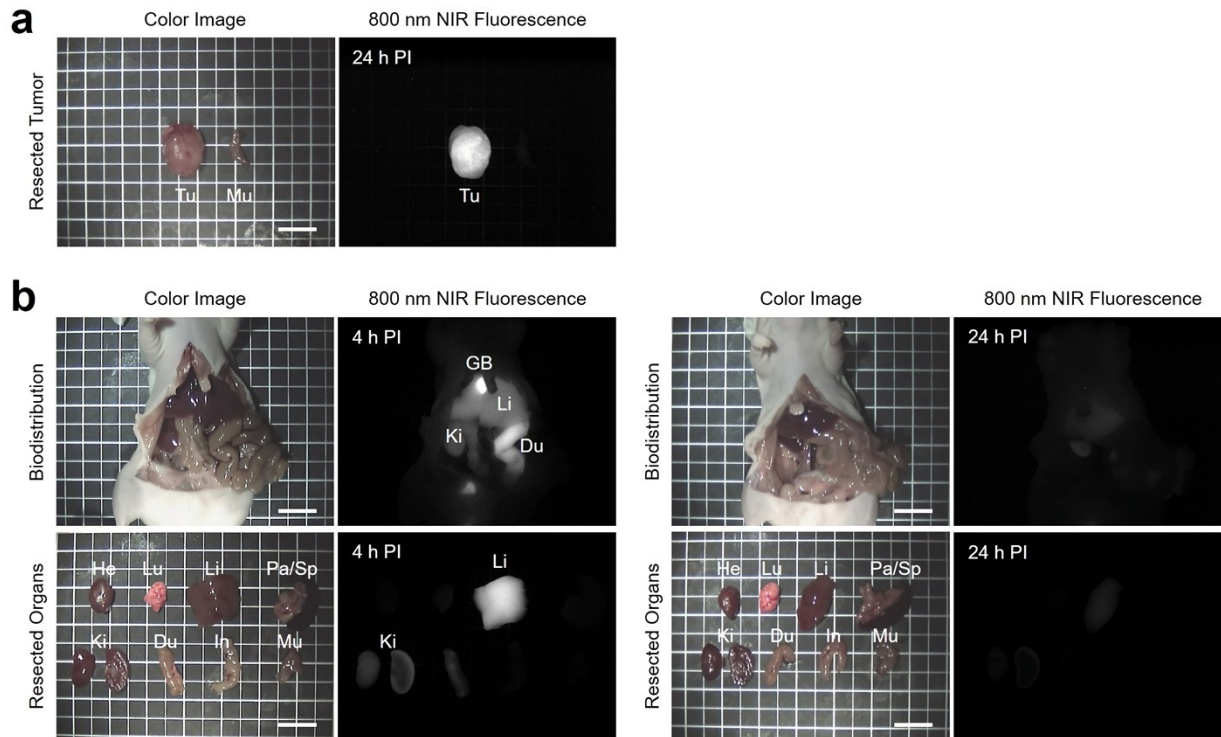


**Fig. S3** Time-dependent biodistribution of CA800SO3 NIR fluorophore. (a) NIR fluorescence imaging of resected tumor at 24 h post-injection of CA800SO3. (b) Biodistribution and resected

organs imaged at 4 h and 24 h post-injection of CA800SO<sub>3</sub>. Tumor mice were intravenously injected with 10 nmol CA800SO<sub>3</sub> and imaged over a certain period of time. Abbreviations: Du, duodenum; GB, gallbladder; He, heart; In, intestine; Ki, kidneys; Li, liver; Lu, lungs; Mu, muscle; Pa, pancreas; Sp, spleen; Tu, tumor; and PI, post-injection. Scale bars = 1 cm. Images are representative of three independent experiments. All NIR fluorescence images have identical exposures and normalizations.

## References

- 1 H. S. Choi, K. Nasr, S. Alyabyev, D. Feith, J. H. Lee, S. H. Kim, Y. Ashitate, H. Hyun, G. Patonay, L. Strekowski, M. Henary and J. V. Frangioni, *Angew. Chem. Int. Ed.*, 2011, **50**, 6258–6263.
- 2 H. Hyun, M. W. Bordo, K. Nasr, D. Feith, J. H. Lee, S. H. Kim, Y. Ashitate, L. A. Moffitt, M. Rosenberg, M. Henary, H. S. Choi and J. V. Frangioni, *Contrast Media Mol. Imaging*, 2012, **7**, 516–524.
- 3 S. Lee, J. S. Jung, G. Jo, D. Jo, D. H. Yang, Y. S. Koh and H. Hyun, *Cancers*, 2019, **11**, 1286.
- 4 Y. Jiang, P. K. Upputuri, C. Xie, Z. Zeng, A. Sharma, X. Zhen, J. Li, J. Huang, M. Pramanik and K. Pu, *Adv. Mater.*, 2019, **31**, 1808166.
- 5 D. Cui, J. Huang, X. Zhen, J. Li, Y. Jiang and K. Pu, *Angew. Chem. Int. Ed.*, 2019, **58**, 5920–5924.
- 6 H. Hyun, M. H. Park, E. A. Owens, H. Wada, M. Henary, H. J. M. Handgraaf, A. L. Vahrmeijer, J. V. Frangioni and H. S. Choi, *Nat. Med.*, 2015, **21**, 192–197.